Synthesis of Water-Soluble Oligomers From Imidazole, Ethyleneglycol Diglycidyl Ether, and Methacrylic Acid. An Insight Into the Chemical Structure, Aggregation Behavior and Formation of Hollow Spheres[a]

Lucía V. Lombardo Lupano, Juan M. Lázaro-Martínez, Nora M. Vizioli, Dimas I. Torres, Viviana Campo Dall' Orto*

The synthesis of non-soluble polyampholytes was modified to obtain water-soluble oligomers, by a sequential reaction at 60 °C of imidazole (IM), ethyleneglycol diglycidyl ether (EGDE) and methacrylic acid (MAA). The hydrogel Poly(EGDE-IM) with disubstituted imidazole (IM^+) residues, enhanced its solubility in water by functionalization with Poly(MAA). NMR and mass spectrometry evidenced ester groups, Poly(MAA) chains, Poly(EGDE), and IM^+ links. Capillary electrophoresis evidenced populations with positive net charge at pH lower than 9, due to IM^+ and protonatable residues (IMH^+). Water-soluble aggregates of oligomers were detected by size exclusion chromatography. The product aggregated with cations such as Fe(II) adsorbing anionic compounds, and formed hollow spheres when citric acid was present.

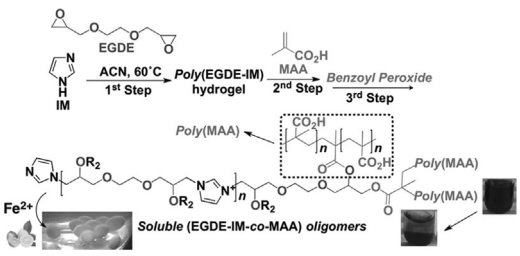

1. Introduction

Polymers and oligomers, bearing a mixture of positively and negatively charged monomer subunits, belong to smart materials with response to temperature, pH, ionic strength, water–organic solvent composition, electrical field, among other stimuli.[1] A characteristic feature of those so called polyampholytes (in particular those composed of weak acid and base species) is that they possess an isoelectric point (IEP) defined as the pH at which the polyampholyte is electrically neutral.[1]

It is known that block polyampholytes (where homopolymer subunits are linked by covalent bonds) in solution behave different from random polyampholytes. Depending on the block length ratios and solubilities, such polymers form large molecular aggregates of well-defined size micelles with a core formed by the oppositely charged

V. Campo Dall' Orto, L. V. Lombardo Lupano, N. M. Vizioli, D. I. Torres
IQUIFIB-CONICET. Junín, 956 (1113) CABA, Argentina
E-mail: vcdall@ffyb.uba.ar
J. M. Lázaro-Martínez
CONICET, Av. Rivadavia 1917 (1033), CABA, Argentina &
Departamento de Química Orgánica, Facultad de Farmacia y Bioquímica, Universidad de Buenos Aires, Junín, 956 (1113) CABA, Argentina
N. M. Vizioli, V. Campo Dall' Orto
Departamento de Química Analítica y Fisicoquímica, Facultad de Farmacia y Bioquímica, Universidad de Buenos Aires, Junín, 956 (1113) CABA, Argentina

[a]**Supporting Information** is available from the Wiley Online Library or from the author.

blocks and a corona with part of the higher charged block.[2–4] The stabilizing factor which prevents the formation of infinite aggregate with increasing polymer concentration is the electrostatic repulsion between molecules if they carry the net uncompensated charge.

These functionalized polymers have found application in areas such as manufacture of lithographic films, drag reduction, ion adsorption, membrane-based bioseparations, cryoprotection, manufacture of water-based coatings, papermaking, skin care, controlled drug release, and tissue engineering.[5–10]

The physico-chemical properties and therefore the applicability of these polymeric materials have been proved to be related to the cationic groups to anionic groups ratio in the resulting product, the density of charged groups in the network, and the cross-linking degree of the chains,[1,11] as expected. In this sense, a huge variety of practical examples evidence the dependence of the resulting polymeric properties on the rational functionalization of the network about the proportion of ionizable groups.

Zwitterionic hydrogels, betaines, and mixed charge system containing a homogeneous molecular level mixture of positively and negatively charged regions have demonstrated non-fouling characteristics, i.e., the elimination of non-specific protein adsorption.[11–13]

There are many successful examples where the resulting features of the polymeric material are strongly related to the proportion of ionizable functional groups in the feed ratio. Using the one-pot synthetic strategy of random copolymerization, our group has previously obtained non-soluble polyampholytes by mixing methacrylic acid (MAA) with imidazole (IM) or derivatives around the charge balance point at high concentration, plus the addition of ethyleneglycol diglycidyl ether (EGDE).[14–17] The epoxy groups of the last monomer were opened up by both carboxylic groups of MAA and the pyridine-type nitrogen of the *N*-heterocycle, and a peroxide-initiated radical polymerization of MAA segments covalently bound to EGDE finally gave a statistical copolymer, non-soluble in water. This copolymer was obtained as a monolith that swelled in contact with water, and could be milled into particles. When different functionality ratios were tested, the synthesis did not succeed.

The final distribution and density of the functional groups promoted the adsorption of proteins and ionic compounds with considerably high loading capacity.[18,19] This result particularly contrasted the expected anti-fouling feature mentioned above: in our development, the homogeneous molecular level of positive and negative charges in the feed mixture enhanced protein adsorption. The uptake of biomolecules was observed at pH values above the IEP, where both molecules (polyampholyte and protein) bore negative net charge.[15,19] The presence of positive and negative domains in both compounds would account for an interaction between dipoles. In this case, desorption took place in saline medium, evidencing the electrostatic nature of the binding. Nevertheless, the release of protein from polyampholyte—protein associates can take place at the IEP of polyampholytes due to realization of the "isoelectric effect," that is if the cooperativity of the intrachain interaction of acidic and basic groups within a single macromolecule predominates over those for the interchain interaction.[20]

In this work, we present the results of varying the synthetic strategy on the solubility of the product and on the monomer distribution in the network, keeping the feed ratio, and concentration of the reactive monomers. The innovation consisted in mixing IM and EGDE in a first step making them react at 60 °C, then adding MAA in a second step and incubating at 60 °C for more than 12 h before the radical polymerization induced by benzoyl peroxide. The product separated from the reaction organic solvent, giving a latex-type material soluble in distilled water. A mixture of oligomers was formed in this simple and non-expensive synthetic procedure. In this article, we present the characterization of this product and explore the potential applications: co-precipitation with anionic dyes for textile industrial wastewater treatment, and formation of hollow spheres that dissolve at pH above 7.0.

About the environmental application chosen in this work, we studied the decolorization of aqueous solutions of Direct Blue 273 (DB273), an azo-dye usually employed in paper industry whose decolorization has been recently reported.[21] It is well known that synthetic dyes with azo bonds represent the largest group of industrial colorants produced annually, and are resistant to the biodegradation in aerobic conditions.[22] On the other hand, the azo bond can be reduced by biotreatment in anaerobic conditions, giving rise to aromatic amines which can be toxic and carcinogenic.[23] Here, we make an approach of efficient decolorization by phase separation.

About the preparation of hollow spheres, which consist of organic and inorganic composites, they have attracted considerable attention due to their potential applications in drug delivery, artificial cells, catalysis, and optical sensing, among others.[24–27] This study has demonstrated the possibility of forming hollow spheres by interfacial coordination of the new oligomers with Fe(II)/citric acid in a single step.

2. Experimental Section

2.1. Materials and Reagents

Ethylene glycol diglycidyl ether (EGDE; 50 wt% in ethylene glycol dimethyl ether; MW: 174.197; 12.1% oxirane oxygen; SW: 1.1891) was from TCI America. Imidazole (IM; 99 wt%; MW: 68.077) and methacrylic acid (MAA; 99 wt%; MW: 86.09; SW: 1.015) were purchased from Sigma–Aldrich. Benzoyl peroxide was from Fluka.

Macromol. Mater. Eng. **2015,** DOI: 10.1002/mame.201500276

Acetonitrile from Baxter was of HPLC grade. Direct Blue 273 (CAS number: 76359-37-0; chemical formula: $C_{33}H_{20}CuN_5O_{11}S_3$. 3Na; MW: 891.26) was from Clariant. Water was distilled with a FIGMAY glass apparatus (Córdoba, Argentina). All other reagents were of analytical grade.

2.2. Instruments

High-resolution ^{13}C solid-state spectra for the polymers were recorded using the ramp $^1H \rightarrow {}^{13}C$ CP-MAS (cross-polarization and magic angle spinning) sequence with proton decoupling during acquisition. All the solid-state nuclear magnetic resonance (ss-NMR) experiments were performed at room temperature in a Bruker Avance II-300 spectrometer equipped with a 4 mm MAS probe. The operating frequencies for protons and carbons were 300.13 and 75.46 MHz, respectively.[28] The solution NMR experiments were performed in a Bruker Advance II-500 spectrometer. Different number of scans was performed for the acquisition of the ^{13}C-NMR spectra in the samples.

The FTIR spectra of the polymers and their complexes were recorded on a Nicolet 380 spectrometer using KBr pellets, or Smart Multi-Bounce HATR (horizontal attenuated total reflexion) with ZnSe crystal and 45° angle of incidence (4000–650 cm^{-1}) for solutions or non-crystalline samples. Elemental analysis was performed with a Carlo Erba EA 1108 device. Potentiometric titrations of three synthesis batches of the polymer were carried out in triplicate with a HANNA Instrument pH meter model HI 8424 supplied with a combined glass electrode, using HCl standard solution as titrant after deprotonation with 0.1 M NaOH. UV–visible spectra were obtained with an Evolution Array UV–visible Spectrophotometer Thermo Scientific.

Capillary electrophoresis separations were performed in a P/ACE MDQ (Beckman Coulter, Brea, CA, USA), equipped with a UV–VIS absorbance detector. Data were processed by 32 KaratTM software (Beckman Coulter).

Zeta potential measurements were performed with a Zeta Potential Analyzer ZetaPlus from Brokhaven Instruments Corporation, as a function of pH at 25 °C and constant ionic strength of 10^{-3} M KCl. Dynamic viscosity was measured with a Brookfield DV-II+ device, at different pH values.

For size exclusion chromatography (SEC) in aqueous medium, a Waters HPLC system connected to a Waters 2414 (model 410) differential refractometer was used at 30 °C. A set of three columns Ultrahydrogel (Waters, 7.8 × 300 mm^2) was used; pore sizes: 120–250–500 Å; fraction limits: 5×10^3, 8×10^4, and 4×10^5 $g \cdot mol^{-1}$. Volumes of 20 μL samples were injected by a Model 7010 Rheodyne injector; the flow rate was 0.8 $mL \cdot min^{-1}$.

Ultraviolet matrix-assisted laser desorption–ionization mass spectrometry (UV–MALDI MS) was performed on the Bruker Ultraflex Daltonics Time-of-Flight/Time-of-Flight (TOF/TOF) mass spectrometer (Leipzig, Germany).

2.3. Synthesis of Water-Soluble (EGDE-IM-co-MAA) Oligomers

The reaction proceeded without stirring, except when some reagent was added. In a first step, an aliquot of 6.0 g (88 mmol) of IM was dissolved in 24 mL of acetonitrile in a round-bottom flask. Then, 12 mL of EGDE (108 mmol oxirane oxygen) was added to the mixture, the end of the neck was covered with a piece of aluminum foil and it was thermostatted at 60 °C for 24. It must be pointed out that the mixture was not deoxygenated. In a second step, 6.0 mL of MAA (71 mmol) was poured into the mixture and the reaction continued for other 24 h at 60 °C. In a third step at 60 °C, aliquots of 0.2 and 0.3 g of benzoyl peroxide were added, the solution becoming opalescent and a white elastic material separating from the solution. The reaction was brought at room temperature after 60 min, the supernatant was discarded and the solid was washed with three portions of acetonitrile. Then, the solid product was slowly dissolved in a minimum volume of distilled water to obtain solutions of around 300 $mg \cdot mL^{-1}$, determined by lyophilization and weight. Some fractions of the solutions obtained from the different production batches were dialyzed against distilled water, using 12 kDa-cutoff cellulose bags from Sigma–Aldrich.

2.4. NMR Experiments

The bulk product was studied by ^{13}C CP-MAS and by solution-NMR. Besides, an aliquot of 0.15 g of (EGDE-IM-co-MAA) oligomers dissolved in 5.0 mL of water was mixed with 2 mL of methanol or 2 mL of acetonitrile. Fractions of the material precipitated in both cases and were dried at room temperature. ^{13}C CP-MAS spectra were obtained for characterization of the organic solvent-aggregated fractions.

The product precipitated with acetonitrile slowly redissolved in D_2O, and the solution was used for the ^1H NMR and ^{13}C NMR spectra. The product precipitated with methanol could not be redissolved in water.

2.5. Capillary Electrophoresis Analysis

The native and the dialyzed solutions were then analyzed by capillary zone electrophoresis (CZE) in order to determine the eventual presence of monomers, and the net charge of the different populations of products as a function of pH.

Separation conditions: background electrolyte (BGE): 0.050 M sodium phosphate, pH: from 4.0 to 9.0; capillary: fused silica (Polymicro Technologies, Phoenix, AZ, USA) of 50 mm id × 365 mm od, 31 cm in length (effective length 21 cm); applied voltage: 5 kV, normal polarity; sample introduction: 5 s at 3.45 kPa; detection: 214 nm; electroosmotic flow (EOF) marker: 5×10^{-3} M dimethylformamide (DMF); system temperature: 25 °C. Between runs, the capillary was washed with water for 3 min, and BGE for 3 min.

2.6. Size Exclusion Chromatography (SEC) in Water

The mobile phase, 0.050 M tris(hydroxymethyl) aminomethane (TRIS) buffer containing 1.00 M (mobile phase I: MPI) or 0.10 M (mobile phase II: MPII) KCl at pH 8.5 was freshly prepared and filtered through 0.45 μm Millipore nylon filter prior to use. Volumes of 2 mL of 10 mg mL^{-1} product solutions were prepared by diluting the samples in the mobile phase. The product samples were filtered once through 0.2 μm Millipore nylon filters.[29] The molecular weight calibration curve was performed with pullulan standards.

2.7. UV-MALDI MS Experiments

They were performed with three matrixes: 9H-pyrido[3,4-b]indole, norharmane, nHo (Sigma–Aldrich): 1 mg · mL^{-1}, acetonitrile:water (1:1); α-cyano-4-hydroxycinnamic acid, CHCA (Sigma–Aldrich): 1 mg · mL^{-1}, acetonitrile:water. 0.1% trifluoroacetic acid (3:7); 2,5-dihydroxybenzoic acid, gentisic acid, DHBA (Sigma–Aldrich): 1 mg · mL^{-1} water. The sample dilutions tested were 1/10, 1/100, and 1/1000.

2.8. Decolorization of DB273 Solutions

A DB273 solution of absorbance close to 1.0 was prepared in distilled water from the concentrated commercial solution, reaching a concentration of 76 μM DB273 (8.1 mg or 9.1 μmol in 120 mL). An aliquot of 55.4 mg of dissolved (EGDE-IM-co-MAA) oligomers was mixed under stirring. After the addition of 2 mmol (111.7 mg) of Fe(II) from $FeSO_4$ solution, aliquots of the sample at different times were centrifuged, and the absorbance of the supernatant was monitored at 588 nm. A control was made with 300 mg of IM monomer instead of the oligomer sample. Besides, in additional control experiments, each reagent was alternatively replaced by distilled water.

2.9. Hollow Spheres Preparation

Citric acid was dissolved in 0.1 M NaOH solution to make a 1 M solution of pH 2.1. An aliquot of 1 mL of 1 M citric acid/monobasic citrate was mixed with 0.1 mL of 0.1 M $FeSO_4$ solution. Then, a 300 g · L^{-1} oligomer solution was added drop wise to the mixture, to form hollow spheres.

3. Results and Discussion

3.1. Synthesis

EGDE, IM, and MAA were combined to obtain the water-soluble product mixture. As it will be demonstrated in this work, this mixture is mainly constituted by oligomers. The particular features of the first and second steps of synthesis determined the differences in solubility between the former polyampholytes and this new material.

3.1.1. First Step

This initial step in the synthesis of (EGDE-IM-co-MAA) oligomers started with the reaction of EGDE with IM for 24 h at 60 °C to form the Poly(EGDE-IM) hydrogel,[16,30] after the opening of the epoxy groups present in the EGDE molecules by the nucleophilic character of the nitrogen in the IM molecule (Scheme 1). A detailed ATR-FTIR analysis, which evidences structural changes in the IM molecule attributed to its covalent binding to the network, is presented in Figure 1, Figure S1, and Table S1 in Supplementary data.

It is important to mention that N_1-monosubstituted (IM) and N_1-N_3-disubstituted (IM^+) IM units are respectively generated with a transient or permanent positive charge during the process. The N_1-monosubstituted IM units can be protonated with acidic solutions giving rise to IM protonated species (IMH^+), which are pH-sensitive.

At this point, the previously reported synthesis of Poly(EGDE-MAA-IM) (a non-soluble polyampholyte)[16] and the synthesis of Poly(EGDE-IM) should be compared. In the first case, since IMH^+MA^- ion pairs are formed prior to EGDE addition, polyetherification is faster than adduct formation due to the low concentration of IM monomer.[30] The higher amount of polyether leads to polyampholytes that are non-soluble in most solvents.[14–16] Instead, when the Poly(EGDE-IM) hydrogel is synthesized, adduct formation (Scheme 1, stage A) prevails over polyetherification (Scheme 1, stage B), bringing a highly solvated integral polyelectrolyte with positive electric charge even at pH 11.0 due to disubstituted IM (IM^+) units.[16]

3.1.2. Second Step

Then in a second step, the addition of MAA to the Poly(EGDE-IM) mixture at 60 °C was the key of the synthetic process. If the reaction was carried out for less than 12 h, the final product was non-soluble in water; but if the heating was longer than 12 h and followed by the third step (addition of benzoyl peroxide, Scheme 1), a water-soluble product was produced. Thus, in our experiments, incubation was carried out for 24 h, followed by ATR-FTIR analysis (Figure S2 in Supplementary data).

After the addition of the MAA monomer, the faster reaction was the formation of a ionic pair between MAA and IM (acid–base reaction with free monomer or with monosubstituted IM moieties in the Poly(EGDE-IM) hydrogel), and the slower reactions were the opening of the remaining epoxy groups to form esters of MAA, in parallel with the esterification of the hydroxyl groups in the Poly(EGDE-IM) hydrogel by the carboxylic acid of MAA.

Here, the dispersion of the MAA monomer in the Poly(EGDE-IM) contributed to the water solubility of the final product after the polymerization of the MAA segments with the addition of benzoyl peroxide. Thus, the correct functionalization of the positive network with negative domains from Poly(MAA) is fundamental only when some of the MAA monomers are chemically bound to the hydrogel. Otherwise, the non-soluble character of Poly(EGDE-IM) would prevail, even when free monomers of MAA still remained in the reaction mixture for less than 12 h.

3.1.3. Third Step

The third step consisted in the addition of benzoyl peroxide at 60 °C to initiate the radical polymerization of vinyl groups from MAA residues. In this step, the significant variables were as follows: temperature, convection, and amount of peroxide. As it is well known, if the temperature

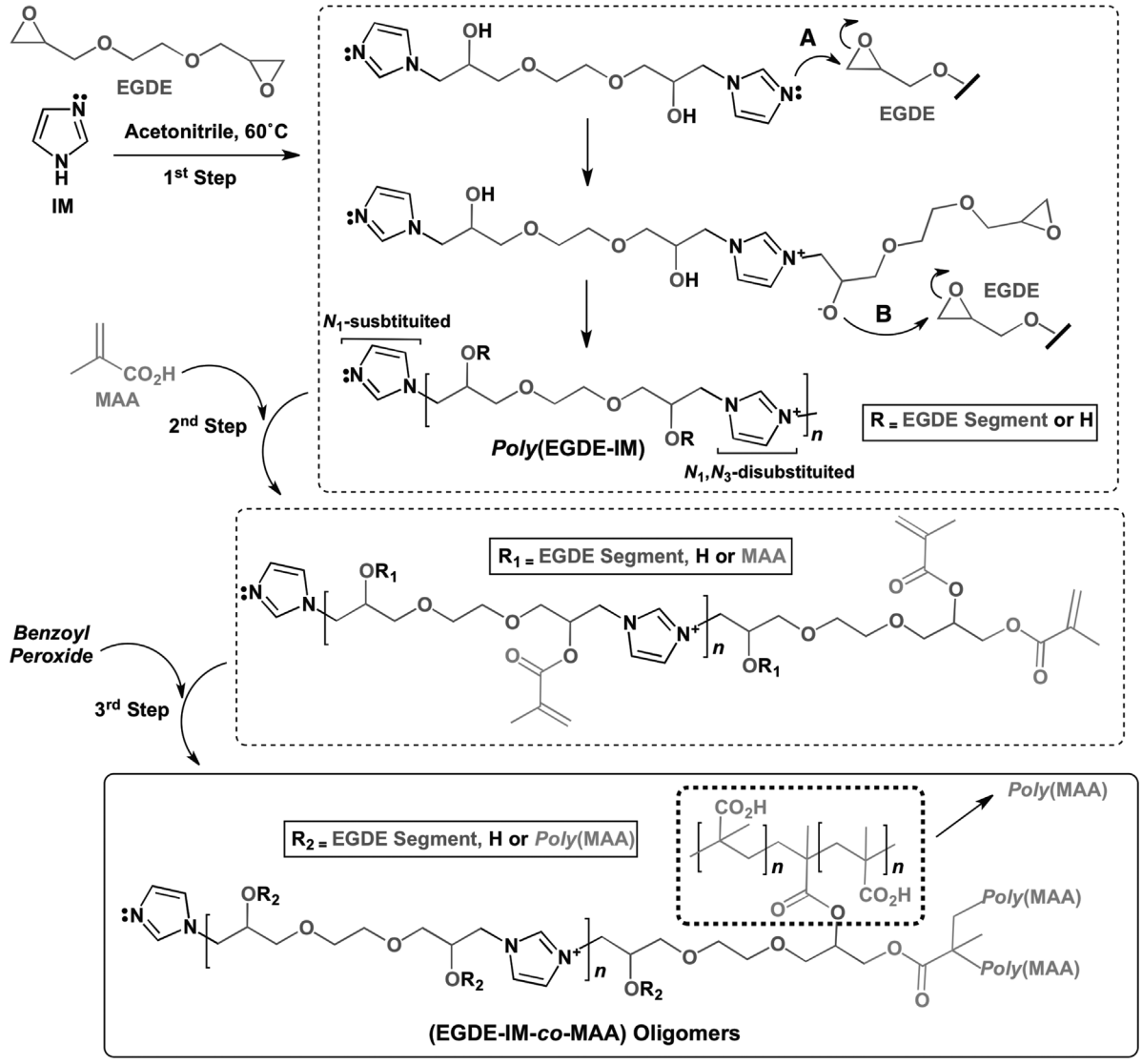

Scheme 1. Synthesis of the water-soluble (EGDE-IM-co-MAA) oligomers.

is below 60 °C and the peroxide is at low proportion (and thus the sample is not deoxygenated), the radical polymerization does not start. In addition, the opalescence as initial evidence of the chemical reaction was only observed in the absence of stirring.

The final reaction mixture was kept at 60 °C for 60 min, meanwhile the network grew and separated from the solvent. The liquid was finally drained and the solid was washed with three portions of acetonitrile to remove the remaining monomers. The solid was then analyzed by ATR-FTIR: the bands of vinyl groups from MAA (806, 942, and 1630 cm^{-1}) were affected (Figure S2 and S3 in Supplementary data). The solid product was finally dissolved in the minimum amount of water, reaching concentrations of 300 $mg \cdot mL^{-1}$.

Yield, determined by lyophilization of the aqueous solution and weigh of the solid, was around 43%. The elemental analysis of the bulk product presented in Table S2 in Supplementary data indicates an average amount of 6.0 mmol N $\cdot g^{-1}$ and 3.0 mmol IM g^{-1}. Besides, the percentages of the other elements were consistent with a stoichiometry of 3.0 mmol MAA g^{-1}, 2.5 mmol EGDE g^{-1} and 5 mmol H_2O g^{-1} in the final bulk product. It must be pointed out that the composition for the different batches of bulk product and for their acid fractions (Table S2 in Supplementary data) is reproducible.

Scheme 1 summarizes the probable structures obtained at each synthesis step, showing the main functional groups attached to the network of (EGDE-IM-co-MAA) oligomers. Even when equivalent amounts of IM and MAA were found

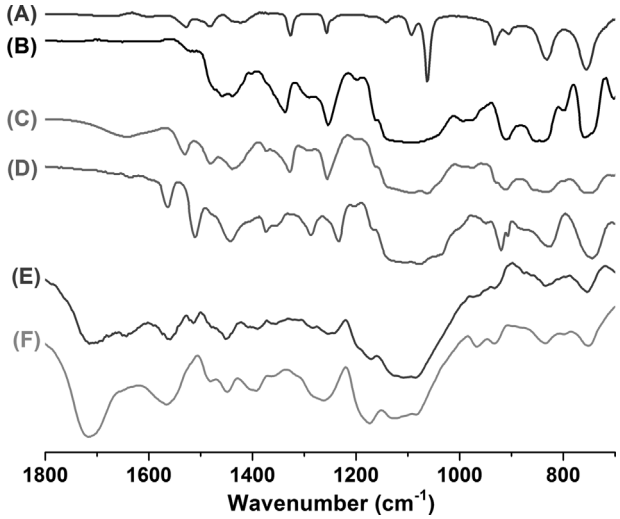

Figure 1. ATR-FTIR spectra of IM (A) and EGDE (B) in acetonitrile, reaction mixture of EGDE and IM in acetonitrile at t: 0 (C) and at t: 24 h (D) at 60 °C. Pellet FTIR of bulk (EGDE-IM-co-MAA) oligomers (E) and hollow spheres (F).

in the bulk product, a mixture of networks with different block ratios was obtained, as will be demonstrated in this work.

The ATR-FTIR spectrum of this oligomeric material (from a three-step synthesis) was compared with the spectrum of the non-soluble polyampholyte Poly(EGDE-MAA-IM) obtained in the one-pot synthetic strategy (Figure S3 in Supplementary data). The profile was similar in both cases, indicating that the functional groups bound to the networks were the same even if the solubility of each material depended on the synthetic strategy.

3.2. NMR Characterization

The material was structurally characterized by solution- and ss-NMR experiments. First, to analyze different product fractions raised from the synthetic process, the bulk (EGDE-IM-co-MAA) oligomers were precipitated with acetonitrile or methanol and both solids were characterized by ss-NMR techniques. Then, the solids were treated with D_2O to be studied by solution-NMR; however, it was possible to re-dissolve and study only the aggregate from acetonitrile. The ^{13}C CP-MAS spectra (Figure 2I) of the solids obtained presented similar signals associated with the corresponding monomers. The polymerized MAA segments were at 17.1 (CH_3–, C_6), 45.7 (>C<, C_5), 55.9 (–CH_2–, C_4), and 183.8 ppm (–CO_2H, C_1 and –CO_2R, C_2), and the IM moieties at 123.8 (N–CH=CH–N, C_8) and 137.8 ppm (N=CH–N, C_7) covalently bound to the EGDE segments at 51.2 ppm (N–CH_2–EGDE, C_9). The rest of the EGDE signals can be observed at 70.6 ppm (–CH_2–O– and >CH–O–, C_3).

An important structural difference between this new material and previous hydrogel materials was that the chemical shifts of the carbons of the carboxylic acid and ester groups in (EGDE-IM-co-MAA) oligomers were overlapped at 183.8 ppm and there were not two well-resolved signals at 180.0 and 185.0 ppm as those observed in the non-soluble polyampholyte Poly(EGDE-MAA-IM) obtained in the one-pot synthetic process (Figure S4 in Supplementary data).[16] This indicates that the environments of these carbons were modified by this new methodology.

The solid obtained from methanol (spectrum C in Figure 2I) presented a significant decrease in the signals coming from the IM and EGDE segments, whereas the polymerized MAA regions were practically not affected, when compared with the bulk material or the solid obtained from acetonitrile (spectra A and B in Figure 2I). Even when ^{13}C CP-MAS experiments are not quantitative, the ^{13}C CP-MAS spectra were acquired in the same conditions and the reduction of all the signals coming from the EGDE and IM ($C_{3–7–8–9}$) was affected in the same way, since the IM residues are only bound to the EGDE segments. These behaviors explain the solubility or insolubility in water of the corresponding solids from acetonitrile or methanol, indicating that the higher content of polymerized MAA segments is the main reason of insolubility in methanol and evidencing that the synthetic process produced at least two significant populations: one with a lower content of polymerized MAA segments (soluble in water, after being precipitated with acetonitrile) and the other with a higher content of polymerized MAA segments (non-soluble in water, after being precipitated with methanol).

Then, the bulk (EGDE-IM-co-MAA) oligomers and the soluble fraction in D_2O (from acetonitrile) were studied through solution-NMR spectroscopy, and the results are shown in Figure 2II and **3**. The ^{13}C- and ^{1}H-signals were unequivocally assigned by comparison with 2D-NMR experiments previously reported in similar materials[16] since, in the ^{13}C solution-state NMR, the signals corresponding to the polymerized MAA segments (C_4 and C_5) were shifted and the quaternary carbon (C_5) was decreased in comparison with the solid-state spectrum (Figure 2). In the ^{13}C-NMR in D_2O, the resolution of the NMR signal was increased and two-well resolved signals corresponding to the carbonyl groups C_1 and C_2 were observed. The inset in the ^{13}C-NMR spectrum for the bulk oligomer in D_2O clearly shows the visualization of the C_4 and C_5 signals (Figure 2II). In addition, the ^{13}C-NMR spectrum of the bulk oligomer in D_2O presents a higher number of resonance signals coming from the imidazole moieties ($C_{7–8}$) together with the methylene carbons of the EGDE segments bound to the nitrogen of the imidazole rings (C_9), in contrast with the ^{13}C-NMR spectrum of the material precipitated with acetonitrile, where C_9 and $C_{7–8}$ were particularly affected. These

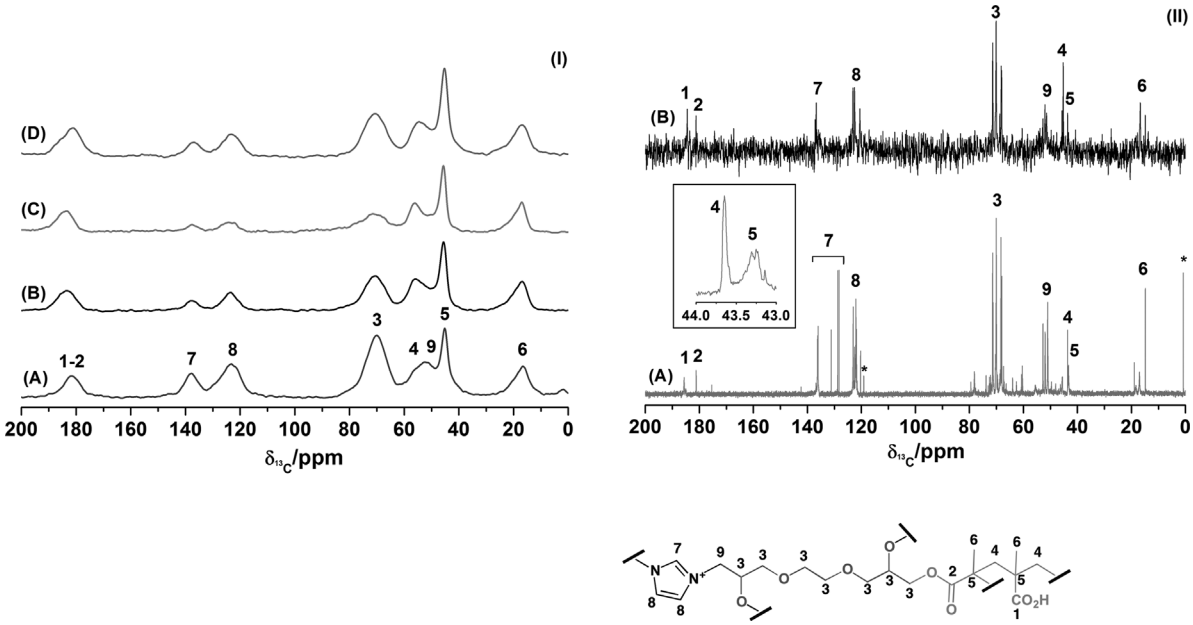

Figure 2. ^{13}C CP-MAS spectra for the bulk (EGDE-IM-co-MAA) oligomers (A), precipitated material with acetonitrile (B) or with methanol (C) from an aqueous oligomer solution. Hollow spheres material (D) (I). ^{13}C-NMR spectra for the bulk (EGDE-IM-co-MAA) oligomers in D_2O (A) and the precipitated material with acetonitrile from an aqueous oligomer solution and then dissolved in D_2O (B) (II). The residual of acetonitrile signals are indicated with asterisks.

observations are related to important differences observed at around 7–9 ppm in the ^1H-NMR spectra for the bulk oligomer and the material precipitated with acetonitrile, being indicative that there are at least two significant oligomer domains in terms of chemical structure that can be clearly studied and characterized from the solution- and solid-state NMR spectra (Figure 2 and 3).

Also, the ^1H-NMR spectrum in Figure 3 shows the signals corresponding to the different segments that form (EGDE-IM-co-MAA) oligomers; the protons corresponding to the IM (N=CH–N and N–CH=CH–N, H_{7-8}), EGDE (–CH_2–O– and >CH–O–, H_3), and polymerized MAA (–CH_2–, H_4/CH_3–, H_6) segments were at 7.58–7.42, 3.51–3.72, and 1.80/1.05 ppm, respectively.

The H_9 in Figure 3 corresponds to protons of the methylene bound to the IM ring at 4.27–4.40 ppm after the opening of the epoxy groups in the EGDE molecules. In particular, the ^1H resonance lines corresponding to the methyl and methylene of the polymerized MAA segments were broadened due to the heterotactic and syndiotactic configurations.[31] In addition, it was possible to estimate that the monomeric composition of the bulk oligomer and the material precipitated in acetonitrile was 1.1:1.0:1.2 and 1:1:2, respectively, in terms of IM:EGDE:MAA. With these evidences, the relative polymerized MAA content was higher when the material was precipitated in acetonitrile; however, the bulk oligomer material presented a similar relative content of each monomer. Also, the remaining non-polymerized MAA monomers were lower than 0.05%, having into account the characteristic proton resonance lines at 5.59 and 5.28 ppm (indicated with asterisks in Figure 3). In the ^{13}C-NMR or ^{13}C CP-MAS spectra, the signals corresponding to the non-polymerized MAA monomers could not be observed due to the lower sensitivity of these experiments.

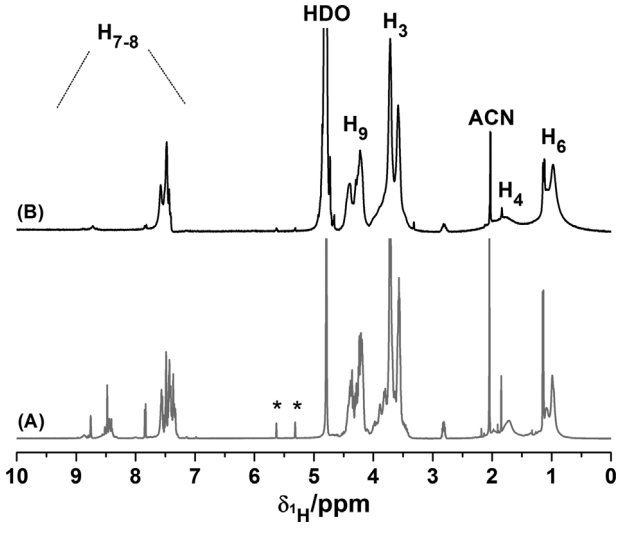

Figure 3. ^1H-NMR spectra for the bulk (EGDE-IM-co-MAA) oligomers in D_2O (A) and precipitated material with acetonitrile from an aqueous oligomer solution and then re-dissolved in D_2O (B). The residual of acetonitrile is indicated as ACN.

3.3. Capillary Electrophoresis

The aqueous solution behavior of oligomers bearing acid and basic groups is dictated by Coulombic interactions between anionic and cationic species located on different monomer units. Capillary zone electrophoresis (CZE) is a powerful and simple tool to characterize the charge density of soluble polymers[32] even if the polymerization degree and hydrophobicity clearly affect their electrophoretic behavior.[33]

Samples of the aqueous solutions were dialyzed using 12 kDa-cutoff cellulose bags, to eliminate residues of solvent and eventually of monomers, and then analyzed together with the native non-dialyzed oligomer solutions by CZE with normal polarity at different pH values. The CZE profiles of the oligomers at different pH values in the range between 4.0 and 9.0 exhibited the presence of at least three main bands, which were resolved at pH 7.0 (Figure 4). The band attributed to the most positively charged species ran before the EOF marker (DMF) at all the pH values tested. Considering the equal amounts of MAA and total IM in the bulk mixture, a possible explanation for the positive net charge of an oligomer population even at pH 9.0 is the existence of Poly(EGDE-IM) blocks that are larger than the Poly(MAA) blocks in these molecules, with a preponderance of positive permanent sites.

The other two bands became neutral at a pH close to 8, sharing the retention time (tr) with the neutral marker at pH 9.0.

At pH values between 4.0 and 6.0, a fraction of the oligomer mixture precipitated from the solution and the supernatant was then filtered to be analyzed. A single broad band had a tr shorter than that of DMF, indicating a difficulty to separate the positively charged networks with different mass to charge ratio. Besides, the tr of DMF was significantly affected by the sample, becoming larger with the number of runs. This effect was a strong evidence of the interaction between the positively charged residues on the oligomer and the capillary wall, which tended to minimize the EOF upon charge neutralization.[32]

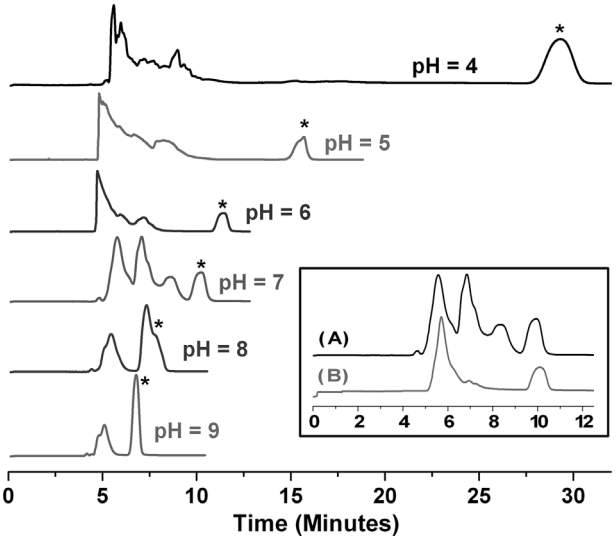

Figure 4. CZE of (EGDE-IM-co-MAA) oligomers soluble fraction in 0.05 M phosphate solution at different pH values. * DMF peak (added neutral marker). Insert: CZE at pH 7.0 of non-dialyzed (A) and 2 d-dialyzed oligomer sample (B). The non-dialyzed solution was diluted 1 in 25 mL (the final concentration at pH 6.0 or higher, was 12 mg · mL^{-1}), and the dialyzed solution was diluted 1 in 2 mL.

When the sample was run in reverse mode at pH 9.0, no peaks were detected at 214 nm during the 70 min of observation. Besides, a standard of 35 mg · mL^{-1} sodium polyacrylate (PA) was analyzed with normal polarity, obtaining a very small peak with a tr longer than that of DMF. The low extinction coefficient of PA (and eventually of polymethacrylate) would explain the absence of bands with negative net charge at alkaline pH in the sample electropherograms, expected for oligomer fractions with an important excess of Poly(MAA) blocks in their structure. Another explanation will be discussed in Section 3.6.

When the non-dialyzed sample was run against a standard of IM monomer, a very small peak was detected at 3.5 min indicating two things: the IM monomer content in the solid bulk product was negligible, and the eventual excess of IM predicted by the yield results remained in the synthesis solvent and was discarded.

The native non-dialyzed sample was compared with the dialyzed product and with the external solution of the dialysis after 24 h of purification: similar CZE profiles were found, indicating that the size of the oligomeric products was below 12 kDa (Figure S5 in Supplementary data). Here, we confirmed that the bulk product was a mixture of oligomers.

3.4. Acid–Base Properties

To study the acid–base properties, the oligomeric material was placed together with a measured excess of an NaOH standard solution. In this condition, the material was considered as an oligomeric base bearing two types of protonatable functional groups ($-COO^-$ and monosubstituted IM residues), and was titrated with an HCl standard solution. When the pH recorded at the titration was close to 6.0, the solution became turbid and some aggregation was observed after additional HCl.

The titration curve is exhibited in Figure 5A: only two inflexion points were obtained for different synthesis batches of this material, suggesting that only an average acid–base behavior was observed. The volumes of the HCl standard solution at the inflection points were used to calculate the density of protonatable sites, which was determined to be 3.6 mmol · g^{-1} (S.D.: 0.3), a value significantly higher than the density of titrable sites in

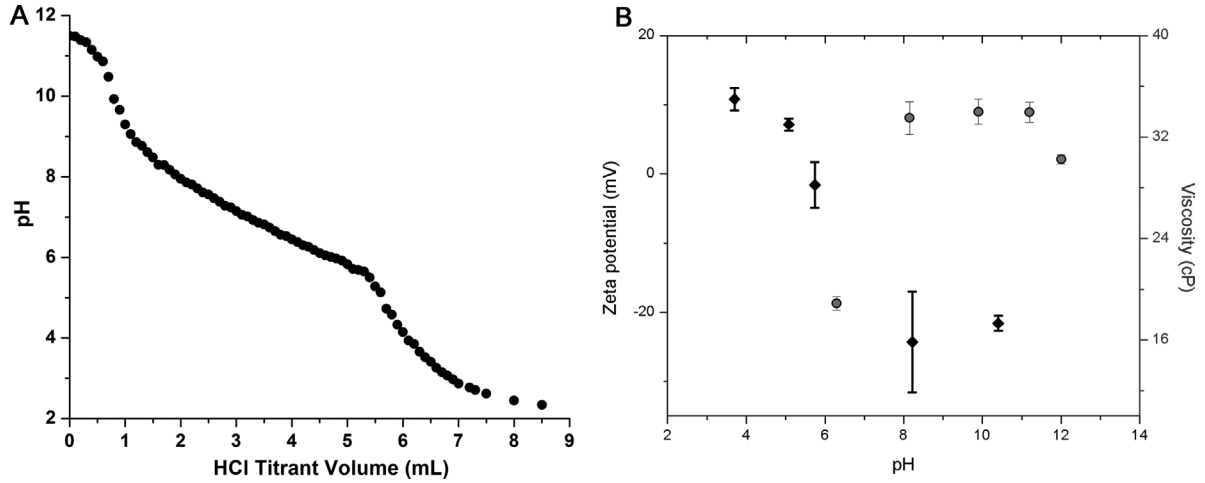

Figure 5. Titration curve of the basic form of (EGDE-IM-co-MAA) oligomers (A). Zeta potential values (◆) and viscosity (●) as a function of pH for (EGDE-IM-co-MAA) oligomers. The oligomer concentration was 15 mg · mL^{-1} for ζ measurements and 200 mg · g^{-1} for viscosity measurements (B).

the non-soluble polyampholyte containing the same monomers.[14–17] Details about the effects of the interaction between charged groups on the apparent acid dissociation constant value are presented in Figure S6 in Supplementary data.

The results of elemental analysis, together with those of NMR and CZE, gave some additional information about the ionizable groups. The integration of ^{1}H-NMR signals of the final oligomeric bulk gave an IM:EGDE:MAA monomer composition of 1.1:1.0:1.2. The elemental analysis showed that the bulk would have 3 mmol of MAA g^{-1} and 3 mmol of IM g^{-1}; the monomer ratio would be IM:EGDE:MAA 1.2:1.0:1.2. Besides, the total sum of fixed sites that could exchange protons should be equal to 3.6 mmol · g^{-1}, meaning that those groups were not completely detected by acid–base reactions. In fact, IM residues could be either monosubstituted (IM) and protonatable (IMH^{+}), or disubstituted with a positive permanent charge (IM^{+}). The fixed IM^{+} could bind OH^{-} as a counterion at the beginning of titration, when NaOH was added but, since the neutralization of this bound OH^{-} could not be distinguished from free OH^{-} by potentiometry, these sites were not included in the 3.6 mmol · g^{-1}. MAA moieties would be part of Poly(MAA), where carboxyl groups would participate in acid–base reactions as well as in ester-type unions with Poly(EGDE-IM) blocks, in accordance with ^{13}C-NMR evidence.

3.5. Zeta Potential, Viscosity, and Studies of Solubility

Although the CZE experiments did not evidence the existence of negatively charged structures, the presence of equivalent amounts of acid and basic groups in the bulk product, together with the spectroscopic evidence of Poly(MAA) blocks, would predict the existence of an IEP for the oligomer mixture. Figure 5B presents the data of zeta potential (ζ) as a function of pH, from which an IEP of 5.7 was estimated for the bulk product.

The ζ spectra obtained at pH close to 6.0 exhibited two signals corresponding to a positive and a negative population. Besides, the spectra obtained below the IEP presented several broad bands at the time that phase separation was evolving, whereas those obtained at pH above the IEP presented a predominant band with negative net charge and a small neutral band.

The viscosity profile as a function of pH between 6.0 and 12.0 followed the same tendency as ζ, with a marked decrease close to pH 6.0 due to the precipitation of an oligomer fraction (Figure 5B).

Although it was possible to detect an IEP by ζ measurements for the bulk material, the solubility as a function of pH indicated that the product was not a polyampholyte but a mixture of oligomers with a variable ratio between acid groups and basic groups.

Lowe and McCormick explained that statistical polyampholytes tend to be soluble at the IEP, whereas block polyampholytes tend to be soluble above and below the IEP, but precipitate at/around this critical pH.[1] Instead, the generic (EGDE-IM-co-MAA) oligomers were soluble only at a pH above 6.0, a stable suspension was formed when the pH was brought between 4.0 and 6.0, and a latex-type solid separated from the solution at a pH below 4.0.

The solubility of the generic (EGDE-IM-co-MAA) oligomers was studied in different environments. Some oligomer fractions aggregated and precipitated from the aqueous

solution under certain experimental conditions such as simple dilution with distilled water, in mixture with methanol or acetonitrile, at pH below 6.0, or in mixture with Fe(II) (Figure S7 in Supplementary data).

Considering all the experimental results, we can conclude that the fractions of product that precipitated by addition of acetonitrile or methanol exhibited a high content of MAA monomer, being even higher for the solid from methanol. This monomer could be involved in the esterification with EGDE residues and/or bound by radical polymerization through vinyl groups. These fractions could also have lower content of IM residues, since the signals at 832 and 1510 cm^{-1} from the heterocycle bound to EGDE were missing (Figure S8 in Supplementary data). These structures with higher proportion of MAA residues are expected to bear negative net charge over a wide pH range (if esterification does not predominate in the network), and were detected by ζ measurements at pH values above the IEP.

No phase separation was observed in alkaline medium. Besides, at pH 9.0 the pKa (negative logarithm of the apparent acid dissociation constant of protonatable sites) of the bulk (EGDE-IM-co-MAA) oligomers was close to 8.0 and the acid dissociation degree (α_1) was 0.92, indicating that the amount of IMH^+ residues would be low. So, the negative charge from $-COO^-$ would be compensated mostly by permanent IM^+ in the oligomer populations that reached neutrality at pH 9.0, detected in CZE measurements (Figure 4 and Figure S6 in Supplementary data). Surprisingly, these neutral molecules remained soluble in aqueous solution at pH 9.0.

When the bulk material was dissolved in water, the pH value varied between 6.2 and 6.5 between synthesis batches. At this pH range, the bulk oligomer had negative net charge with a small ζ but enough to account for the stability of the solution.

At a pH below 6.0, a fraction of the material separated from the solution, meanwhile other fractions remained soluble. Additional information can be found in the elemental analysis depicted in Table S2 in Supplementary data for both the bulk material (lyophilized) and its acid form obtained by precipitation with HCl: the acid fractions exhibited higher proportion of MAA and lower IM residues in the backbone.

To understand this behavior, the probable structure of diblock oligomers (Scheme 1), where the size of the blocks could be different in each particular molecule, should be considered. On the one hand, it is a fact that Poly(EGDE-IM) blocks were formed in the first step of synthesis.[16,30,34,35] Regarding MAA, a fraction of those MAA residues could be involved in ester groups. On the other hand, the estimated pKa of the bulk product was around 6.5 at acid pH, and α_1 was 0.22 at pH 6.0 and 0.14 at pH 5.7 (Figure S6.B and C in Supplementary data), indicating that most free carboxylic groups from MAA would be present in the neutral form, possibly being part of inner H-bridges.[36] This particular conformation in the regions of (relatively) large acid blocks would significantly affect the solubility of a fraction of the oligomeric sample with excess of MAA groups (even though it supported positive charges from IMH^+ and IM^+) and possibly forming regions where the hydrophilicity was substantially diminished. In agreement, it has been reported that the strong interactions between carboxyl groups in polymer chains cause the formation of thick interfacial films in oil-in-water emulsions at low pH values.[37]

The probable structure of the water-soluble diblock oligomers is consistent with the synthetic strategy applied, since IM reacts with EGDE in a first step forming blocks of EGDE-IM adducts, followed by the addition of MAA (where ester groups could be formed) and a final treatment with benzoyl peroxide to polymerize vinyl groups from free and esterified MAA. This structure would be configurationally different from the non-soluble statistic polyampholytes obtained by a one-pot mixture of the reagents and reported in previous articles,[14–16] but keeping most functionalities. In non-soluble polyampholytes, polyetherification would prevail over EGDE-IM adducts.

In summary, although the different populations of oligomers presented asymmetry in the size/length of each constitutive block, it was possible to determine an IEP for the bulk product. Besides, the solid separated from the solution at a pH below 4.0 exhibited an excess of MAA groups, whereas the neutral molecules detected by CZE at a pH above 6.0 were stable in solution.

3.6. Assessment of the Molecular Weight of the Oligomers

Preliminary information regarding the molar mass of all the oligomers was obtained from dialysis: the cellulose bags of 12 kDa-cutoff were permeable to all the oligomeric fractions.

Analysis by size exclusion chromatography (SEC) was performed in aqueous solution according to previous reports for polyampholytes derived from MAA and amine groups.[29] When 10 $mg \cdot mL^{-1}$ oligomer aqueous solutions were injected in the SEC system at pH 8.5, bands around 300–400 $kg \cdot mol^{-1}$ (based on pullulan standards), were detected in two different synthetic batches (Figure S9 and Table 1). These bands were also present in the solutions of the oligomers that had previously precipitated in acetonitrile or methanol.

These results would evidence the formation of water-soluble aggregates of oligomer molecules, being the aggregation number detected (n): 2, 20, 35, and 60, when the smallest peak (15.0 $kg \cdot mol^{-1}$) was taken as a reference.

Table 1. Molecular masses for peaks eluting from SEC column. Mobile phase I (MPI) was 0.050 M TRIS buffer, pH 8.50, 1.00 M KCl; mobile phase II (MPII) was 0.050 M TRIS buffer, pH 8.50, 0.10 M KCl.

		Molar mass ($kg \cdot mol^{-1}$)	
Sample	**Peak**	**MPI**	**MPII**
Batch I	1	344	337
Batch II	1	739	716
	2	414	432
	3	28.3	n.d.
	4	15.0	n.d.
Batch I treated with acetonitrile	1	339	311
Batch I treated with methanol	1	213	n.m.

n.d.: non-detected n.m.: non-measured

During the dialysis, these water-soluble aggregates would break down as a consequence of dilution in the bags, and the single molecules would permeate to the external medium. We also observed that the size of the water-soluble aggregates increased with the age of the solution.

The stability of these soluble aggregates could be affected in CZE experiments, where the samples were analyzed under a 5-kV perturbation (against 145 V in measurements of ζ). It has been reported that in strong electrical fields, the functionalized polymers stretch out to a highly extended form, for which only a small fraction of the material is still organized.[38] This fact could also account for the particular behavior of these samples at pH above the bulk IEP, where positive mobility was observed in some fractions by CZE; further studies must be carried out to completely understand this aspect.

Additional information was provided by MALDI spectra (Figure S10 in Supplementary data). Oligomers in the low mass range at masses between 300 and 900 were detected. Those of m/z: 483, 551, and 607 were particularly abundant. The expected structures were consistent with the proposed mechanism of synthesis, mainly involving reactions such as esterification of MAA monomers with EGDE by epoxy ring opening and esterification of MAA with the –OH groups from EGDE formed after epoxy ring opening. The most abundant peak corresponding to m/z 551 was consistent with an ion pair structure, formed at the second step after the addition of MAA. We can conclude that a fraction of this intermediary compound was not attacked by free radicals at the third step and remained in the mixture as a by-product. The structure of m/z 735 confirmed the existence of less hydrophilic networks due to some extent of polyetherification that occurred when IM monomer concentration decreased in the reaction.

Although larger-mass Poly(EGDE-IM) attached to Poly(MAA) bulk products were not detected by this method, the existence of (EGDE-IM) adducts would account for all the properties described in this manuscript. We must consider that Poly(EGDE-IM) was actually formed in the first step, that the (EGDE-IM) adducts were identified in a previous work[16] by ESI-MS (even if there was no evidence by MALDI), and that positive networks were here detected by CZE.

3.7. Application in Decolorization Processes

The interaction between oligomers and cations can be driven by electrostatic attraction and/or by coordination through electron donor groups attached to the network. The particles arisen from the interaction between Fe(II) and the soluble (EGDE-IM-co-MAA) oligomers (Figure S7IV in Supplementary data) had huge adsorption capacity and affinity for ionic pollutants when they were formed in-situ in the medium to be decontaminated.

We used an anionic azo dye to demonstrate the outstanding efficiency of the in-situ formed Fe(II)-(EGDE-IM-co-MAA) oligomers particles in the removal of the pollutant from its aqueous solution. We chose the azo dye Direct Blue 273 (DB273) as a model of wastewater from the textile industry (Scheme 2). The dye removal was studied on a 76 μM or 67.7 $mg \cdot L^{-1}$ of DB273 solution after the addition of 0.46 $g \cdot L^{-1}$ oligomer solution and 0.017 M of Fe(II). (Figure 6).

A fast decay in DB273 concentration was observed, showing a decrease of 73% after 3.3 min of reaction. The binding to less–accessible sites continued with a pseudo-first order kinetic constant k of 0.041 ± 0.016 min^{-1} until the dye remaining in the solution was 7% of the initial

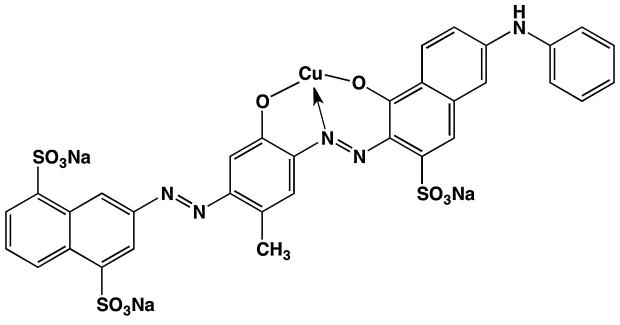

Scheme 2. Chemical structure of Direct Blue 273 (DB273).

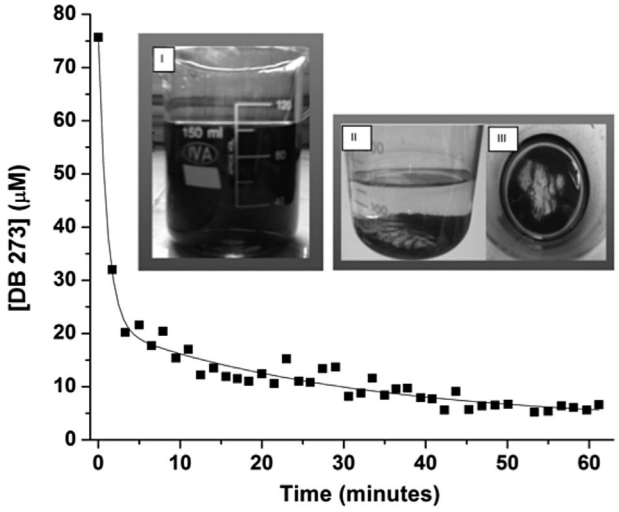

Figure 6. DB273 concentration profile as a function of time, in the presence of (EGDE-IM-co-MAA) oligomers after addition of Fe(II). Insert: images of 76 μM DB273 (I); the suspension obtained in the presence of (EGDE-IM-co-MAA) oligomers and Fe(II) at equilibrium (II and III).

amount. After 55 min, near 93% of the dye was adsorbed on the non-soluble macroaggregates.

Controls made with IM monomer instead of the oligomeric mixture, and replacing alternatively each reagent by water, demonstrated that the interaction between these macromolecules with Fe(II) was necessary for the phase separation (Figure S11 in Supplementary data).

The wastewater depuration was optimized, by reducing almost 400 times the amount of polymer and eight times the amount of Fe(II) required to reach the same efficiency in decolorization obtained in the kinetic experiment, working with a 760 μM DB273 solution. Under these conditions, around 30 mmol (27 g) of DB273 per gram of oligomer was removed from the solution.

This adsorption capacity can be compared with that of non-soluble polyampholytes based on EGDE, MAA, and 2-methylimidazole (2MI).[21] The adsorption obtained experimentally was 280 $mg \cdot g^{-1}$, the maximal estimated by Langmuir model was 403 $mg \cdot g^{-1}$, and that estimated by Dubinin–Radushkevich model was 430 $mg \cdot g^{-1}$. This means that the depuration efficiency was improved 100 times with the in-situ precipitation of the adsorbant.

The Fe(II)-(EGDE-IM-co-MAA) oligomers aggregated material before and after adsorption of DB273 was studied by FTIR (Figure S12 in Supplementary data).

When Fe(II) was used for aggregation, the band at 1510 cm^{-1} shifted to 1522 cm^{-1}. This signal is attributed to vibrational modes of C=N from the IM units when the pyridinic N is protonated, since the band was preserved in the spectrum of both the native bulk material and the acid form. In this case, the shift might be an indication of interaction between the heterocycle and Fe(II). Besides, the signal at 1560 cm^{-1} shifted to 1590 cm^{-1}, possibly due to an interaction of the cation with $-COO^-$ and/or IM residues, and the bands of this composite were clearly more intense and much better resolved than those from the lyophilized or acid form of the polymer, which is expected in a coordination reaction.

The bands corresponding to the main functional groups of the oligomer were not shifted by the adsorption of the dye. Moreover, the bands at 1590, 1448, and 1198 cm^{-1} were more intense in the DB273-Fe(II)-(EGDE-IM-co-MAA) oligomers composite due to the contribution of the stretching vibrational modes of N–H, N=N, and S=O of the dye, respectively.

However, two strong bands from DB273 at 1300 and 1036 cm^{-1}, the first attributed to C–N and the second to the stretching of S=O coming from the sulfonate group, were missing in the composite. This change could be assumed as evidence that the anionic functional groups of the dye interacted electrostatically with the positive sites on the aggregate. The loss of the C–N band could be related to H-bond formation between the dye and the O–H groups of the oligomer.

When DB273 was adsorbed on non-soluble Poly(EGDE-MAA-2MI) particles, the loss of the band at 1300 cm^{-1} was also evident, but the signal at 1036 cm^{-1} could be overlapped to the main signal of C–O–C from EGDE residues.[21] In this sense, we could say that the nature of the interaction of DB273 with the solid particles based on macromolecules derived from imidazolic compounds, MAA and EGDE, was essentially electrostatic combined with H-bond formation.

3.8. Application in Preparation of Hollow Spheres

The oligomers aggregated and precipitated in the presence of a series of metal ions, but formed hollow spheres when Fe(II) was used in combination with citric acid. When Fe(II) was omitted, an amorphous precipitate was formed in the presence of citric acid.

Here, we tested the drop wise addition of a viscous oligomer solution to a less viscous Fe(II)/citric acid solution at pH 2.1 in the formation of interfacial spheres under acidic conditions (Figure 7A–C).

We studied the effect of different concentrations of oligomer and Fe(II)/citric acid solution on the shape and stability of the capsules formed.

The best condition was achieved with a mixture of 0.9 M citric acid/monobasic citrate at pH 2.1 and 9×10^{-3} M $FeSO_4$ solution. A 300 $g \cdot L^{-1}$ oligomeric solution was added drop wise to the mixture using a 1-mL automatic pipette, forming hollow spheres that were mechanically stable in

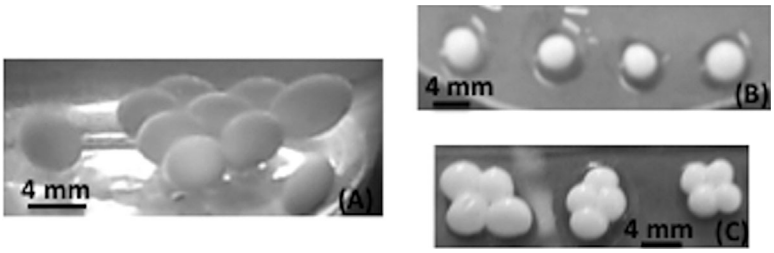

Figure 7. Images of hollow spheres in acid medium (A), and on a glass surface (B and C). The sphere radius as a function of Fe(II) concentration was decreasing from left to right (C).

time. When the experiment was performed with sodium citrate instead of the citric acid/monobasic citrate solution pH 2.1, no spheres were obtained.

The spheres were removed from the solution and cut into two pieces to confirm that they were actually hollow.

Other lower concentrations of Fe(II) and citric acid only formed a cloudy suspension. Higher concentrations of the oligomeric mixture were also tested, but the viscosity was too high to form spherical capsules, resulting in a teardrop-like shape or structures with "tails." In this sense, Driver et al. obtained the same results when one of the polymeric solutions used was too viscous.[27]

The sphere radius decreased as a result of Fe(II) consumption, until the solution became exhausted. As observed in Figure 7C, the spheres on the left were formed with the highest Fe(II) concentration.

When a 1.0 mL aliquot of Fe(II)/citric acid solution was used, four spheres with average radius of 4.0 ± 0.4 mm were obtained. Afterward, the radius decreased by 19% for the next four structures and by 35% for the last four spheres (Figure 7C). At the end of the process, the spheres were too soft to be withdrawn from the solution.

The spheres were dried at 37 °C to be characterized by ss-NMR and FT-IR spectroscopy. These structures collapsed as a consequence of dehydration.

The ^{13}C CP-MAS spectrum for the material of the spheres is seen in Figure 2D. The chemical shifts and relative peak intensities were similar to the profile of bulk (EGDE-IM-co-MAA) oligomers, indicating that the material was included in the structure.

The FT-IR spectrum of the hollow spheres in KBr pellet showed a decrease in the band intensity at 1510 cm^{-1} (Figure 1F) when compared with the spectrum of the bulk material (Figure 1E), indicative of interaction between the heterocycle and Fe(II). The C=O stretching band at 1715 cm^{-1} and the asymmetric stretching of carboxylate at 1570 cm^{-1} were relatively more intense.

The band at 1640 cm^{-1} decreased in intensity when compared with the spectrum of the acid form. This could be due to some loss of inner H-bonds in carbonyl groups from regions of Poly(MAA) now involved in Fe(II) coordination (Figure S8 in Supplementary data).

To analyze the chemical stability, the capsules were transferred to solutions of different pH values at low stirring (60 rpm), resulting completely dissolved at pH 7.0 or higher. These results evidenced the combined effect of interfacial aggregation by protonation of Poly-(MAA) blocks and by coordination of Fe(II) with electron donors from the oligomers. The only presence of Fe(II) or of carboxylic groups was not enough to stabilize the tridimensional network in the sphere.

The mechanical properties of these spheres limit the possibilities of their application in reactors under continuous agitation for biotechnological or environmental applications. This limitation could be related to their relatively large size and could be eventually improved by working on the development of smaller structures.

4. Conclusion

The sequential addition of the reactants and the incubation for more than 12 h before the radical polymerization determined the solubility in water of the oligomers synthesized based on EGDE, IM, and MAA. The first step of the reaction produced the Poly(EGDE-IM) hydrogel, in which the disubstitution of IM moiety originated the permanent positive charge in the molecule. After that, MAA was added to the mixture, forming an ion pair with the basic sites and slowly reacting with the functionalities of the network to form a low amount of ester groups. Finally, the vinyl polymerization of MAA formed polyanionic blocks that remained attached to Poly(EGDE-IM) by means of those esters. The attachment of polyanionic blocks to the Poly(EGDE-IM) gel by means of ester unions was fundamental to enhance the water solubility of the final product. The incubation of Poly(EGDE-IM) with MAA at 60 °C for more than 12 h was necessary to form those ester groups.

The experimental evidence supported the probable chemical structure based on block oligomers, where the size of each block can be variable but always lower than 12 kDa. The solution- and ss-NMR characterization of the bulk (EGDE-IM-co-MAA) oligomers and fractions that precipitated upon organic solvent addition showed the ^{13}C and ^{1}H signals expected for the covalent binding of IM moiety to the EGDE molecule. The findings show that the aromaticity of the heterocycle was preserved and that the oxirane ring was open. The formation of esters between MAA and EGDE was confirmed by ^{13}C-NMR, and also evidenced by MALDI, together with the existence of Poly(MAA) and Poly(EGDE).

It is important to recall that the existence of Poly(EGDE-IM) has been demonstrated in previous works.[14,16] The prevalence of EGDE-IM adduct formation over polyetherification has been studied by ESI-MS, and 500-Da oligomers have been identified in a particular water-soluble fraction.

The enhancement in water solubility at pH values above the IEP could be related to the formation of Poly(MAA) blocks, in association with the higher density of protonatable groups, low degree of polyetherification, the existence of permanent positive charge in oligomers with large Poly(EGDE-IM) to Poly(MAA) blocks ratio, and the possibility of forming highly solvated macro-aggregates.

The soluble oligomers were sensitive to H^+ concentration. When $-COO^-$ groups were neutralized by H^+ at pH values below the IEP, the formation of inner H-bonds between –COOH would account for the decrease in solvation of the chains in large Poly(MAA) blocks attached to smaller Poly(EGDE-IM), leading to the formation of latex-type aggregates.

The properties described in this manuscript could be explained by the asymmetry in the size/length of the constitutive blocks for each oligomeric population present.

The neutral fractions found at pH above 6.0 in CZE experiments would remain soluble, possibly being part of water-soluble macro-aggregates. The formation of these soluble macro-aggregates of oligomer molecules, whose size increased with the age of the solution, was detected by SEC.

Regarding the environmental applicability of this novel material, the Fe(II)-(EGDE-IM-co-MAA) oligomer aggregates presented an extraordinary capacity of anion uptake when precipitated in the presence of an anionic azo dye, representing a potential use of eco-friendly chemistry.

This oligomeric mixture formed hollow spheres when dropped into an Fe(II)/citric acid solution. The combined effect of Fe(II) coordination and oligomer interfacial aggregation determined the morphology of these structures. Their solubility at pH values above 7.0 makes these capsules potentially adequate for intestinal release in drug delivery.

Here, we characterized an oligomeric mixture which was synthesized to be used without further purifications. Additional experiments must be carried out to identify each component of the bulk product for an eventual application of any particular oligomeric fraction.

Appendix

FTIR spectra, ^{13}C CP-MAS spectra, MALDI spectra, CZE electropherograms, potentiometric titration curve, pKa analysis of the oligomer synthetic batches, SEC, viscosimetry, and tables with the results of elemental analysis, FTIR assignments, zeta potential, size of soluble aggregates.the Wiley Online Library or from the author.

Received: July 22, 2015; Revised: August 28, 2015; Published online:DOI: 10.1002/mame.201500276

Keywords: aggregates; capillary electrophoresis; epoxy; NMR; oligomers

[1] A. B. Lowe, C. L. McCormick, *Chem. Rev.* **2002**, *102*, 4177.
[2] N. P. Shusharina, E. B. Zhulina, A. V. Dobrynin, M. Rubinstein, *Macromolecules* **2005**, *38*, 8870.
[3] T. Goloub, A. De Keizer, M. A. C. Stuart, *Macromolecules* **1999**, *32*, 8441.
[4] S. Creutz, M. Garcia, B. Mahltig, M. Stamm, R. Je, *Macromolecules* **2000**, 6378.
[5] W.-C. Wu, C.-Y. Chen, W.-Y. Lee, W.-C. Chen, *Polymer* **2015**, *65*, A1.
[6] K. M. Zurick, M. Bernards, *J. Appl. Polym. Sci.* **2014**, *131*, 40069.
[7] M. Jain, R. Rajan, S.-H. Hyon, K. Matsumura, *Biomater. Sci.* **2014**, *2*, 308.
[8] M. Ladika, T. H. Kalantar, H. Shao, S. L. Dean, J. K. Harris, P. J. Sheskey, K. Coppens, K. M. Balwinski, D. L. Holbrook, *J. Appl. Polym. Sci.* **2014**, *131*, 40049.
[9] Y. Hoshino, H. Lee, Y. Miura, *Polym. J.* **2014**, *46*, 537.
[10] S. E. Kudaibergenov, *Polyampholytes: Synthesis, Characterization and Application*, Kluwer Academic/Plenum Publishers, New York, NY **2002**.
[11] T. Tah, M. T. Bernards, *Colloids Surf. B. Biointerfaces* **2012**, *93*, 195.
[12] T. Zhao, K. Chen, H. Gu, *J. Phys. Chem. B* **2013**, *117*, 14129.
[13] M. E. Schroeder, K. M. Zurick, D. E. McGrath, M. T. Bernards, *Biomacromolecules* **2013**, *14*, 3112.
[14] J. M. Lázaro Martínez, M. F. Leal Denis, V. Campo Dall' Orto, G. Y. Buldain, *Eur. Polym. J.* **2008**, *44*, 392.
[15] M. F. Leal Denis, R. R. Carballo, A. J. Spiaggi, P. C. Dabas, V. Campo Dall' Orto, J. M. Lázaro Martínez, *React. Funct. Polym.* **2008**, *68*, 169.
[16] J. M. Lázaro Martínez, A. K. Chattah, R. M. Torres Sánchez, G. Y. Buldain, V. Campo Dall' Orto, *Polymer* **2012**, *53*, 1288.
[17] J. M. Lázaro Martínez, A. K. Chattah, G. A. Monti, M. F. Leal Denis, G. Y. Buldain, V. Campo Dall' Orto, *Polymer* **2008**, *49*, 5482.
[18] G. J. Copello, L. E. Diaz, V. Campo Dall' Orto, *J. Hazard. Mater.* **2012**, *217–218*, 374.
[19] L. R. Denaday, M. V. Miranda, R. M. Torres Sánchez, J. M. Lázaro Martínez, L. V. Lombardo Lupano, V. Campo Dall' Orto, *Biochem. Eng. J.* **2011**, *58–59*, 57.
[20] S. E. Kudaibergenov, Polyampholytes, in *Encyclopedia of Polymer Science and Technology*, Vol. *101*, John Wiley and Sons Inc., **2008**, pp. 1–30.
[21] P. Y. González Clar, G. Levin, M. V. Miranda, V. Campo Dall' Orto, *Advanced Oxidation Technologies – Sustainable Solutions for Environmental Treatments* (Eds: M. I. Litter, R. Candal, J. M. Meichtry), CRC Press, Taylor and Francis Group, Leiden **2014**, p. 388.
[22] A. B. Dos Santos, F. J. Cervantes, J. B. Van Lier, *Bioresour. Technol.* **2007**, *98*, 2369.
[23] K. T. Chung, C. E. Cerniglia, *Mutat. Res.* **1992**, *277*, 201.
[24] P. Wang, S.-W. Yook, S.-H. Jun, Y.-L. Li, M. Kim, H.-E. Kim, Y.-H. Koh, *Mater. Lett.* **2009**, *63*, 1207.

[25] J. Cui, M. P. van Koeverden, M. Müllner, K. Kempe, F. Caruso, *Adv. Colloid Interface Sci.* **2014**, *207*, 14.
[26] S. J. Dalgarno, N. P. Power, J. L. Atwood, *Coord. Chem. Rev.* **2008**, *252*, 825.
[27] K. Driver, S. Baco, V. V. Khutoryanskiy, *Eur. Polym. J.* **2013**, *49*, 4249.
[28] B. M. Fung, A. K. Khitrin, K. Ermolaev, *J. Magn. Reson.* **2000**, *142*, 97.
[29] C. S. Patrickios, J. A. Strittmatter, W. R. Hertler, T. A. Hatton, *J. Colloid Interf. Sci.* **1996**, *182*, 326.
[30] M. S. Heise, G. C. Martin, *J. Appl. Polym. Sci.* **1990**, *39*, 721.
[31] J. Schriever, J. C. Leyte, *Polymer* **1977**, *18*, 1185.
[32] D. A. Hoagland, D. L. Smisek, D. Y. Chen, *Electrophoresis* **1996**, *17*, 1151.
[33] H. Cottet, P. Gareil, O. Theodoly, C. E. Williams, *Electrophoresis* **2000**, *21*, 3529.
[34] Y. Chen, W. Chiu, K. Lin, *J. Polym. Sci. Part A* **1999**, *37*, 3233.
[35] Y. R. Ham, S. H. Kim, Y. J. Shin, D. H. Lee, M. Yang, J. H. Min, *J. Ind. Eng. Chem.* **2010**, *16*, 556.
[36] K. ElMiloudi, M. Benygzer, S. Djadoun, N. Sbirrazzuoli, S. Geribaldi, *Macromol. Symp.* **2005**, *230*, 39.
[37] M. A. Mironov, I. D. Shulepov, V. S. Ponomarev, V. A. Bakulev, *Colloid Polym. Sci.* **2013**, *291*, 1683.
[38] H. Schiessel, A. Blumen, *J. Chem. Phys.* **1996**, *105*, 4250.